Quantitative ^{68}Ga-DOTATATE PET/CT Parameters for the Prediction of Therapy Response in Patients with Progressive Metastatic Neuroendocrine Tumors Treated with ^{177}Lu-DOTATATE

Claudia Ortega[1], Rebecca K.S. Wong[2], Josh Schaefferkoetter[3], Patrick Veit-Haibach[1], Sten Myrehaug[4], Rosalyn Juergens[5], David Laidley[6], Reut Anconina[1], Amy Liu[7], and Ur Metser[1]

[1]*Joint Department of Medical Imaging, University Health Network, Mount Sinai Hospital and Women's College Hospital, University of Toronto, Toronto, Ontario, Canada;* [2]*Department of Radiation Oncology, Princess Margaret Cancer Centre, University Health Network and University of Toronto, Toronto, Ontario, Canada;* [3]*Siemens Medical Solutions USA, Inc., Knoxville, Tennessee;* [4]*Division of Radiation Oncology, Odette Cancer Centre, Sunnybrook Health Sciences Centre, Toronto, Ontario, Canada;* [5]*Department of Oncology, Juravinski Cancer Centre, McMaster University, Hamilton, Ontario, Canada;* [6]*Division of Nuclear Medicine, St. Joseph's Health Care London, University of Western Ontario, London, Ontario, Canada; and* [7]*Department of Biostatistics, Princess Margaret Cancer Centre, Toronto, Ontario, Canada*

The aim of this study was to determine whether quantitative PET parameters on baseline ^{68}Ga-DOTATATE PET/CT and interim PET (iPET) performed before the second cycle of therapy are predictive of the therapy response and progression-free survival (PFS). **Methods:** Ninety-one patients with well-differentiated neuroendocrine tumors (mean Ki-67 index, 8.3%) underwent ^{68}Ga-DOTATATE PET/CT to determine suitability for peptide receptor radionuclide therapy as part of a prospective multicenter study. The mean follow-up was 12.2 mo. Of the 91 patients, 36 had iPET. The tumor metrics evaluated were marker lesion–based measures (mean SUV_{max} and ratio of the mean lesion SUV_{max} to the SUV_{max} in the liver or the SUV_{max} in the spleen), segmented ^{68}Ga-DOTATATE tumor volumes (DTTVs), SUV_{max} and SUV_{mean} obtained with the liver and spleen as thresholds, and heterogeneity parameters (coefficient of variation, kurtosis, and skewness). The Wilcoxon rank sum test was used for the association between continuous variables and the therapy response, as determined by the clinical response. Univariable and multivariable Cox proportional hazards models were used for the association with PFS. **Results:** There were 71 responders and 20 nonresponders. When marker lesions were used, higher mean SUV_{max} and ratio of the mean lesion SUV_{max} to the SUV_{max} in the liver were predictors of the therapy response ($P = 0.018$ and 0.024, respectively). For DTTV parameters, higher SUV_{max} and SUV_{mean} obtained with the liver as a threshold and lower kurtosis were predictors of a favorable response ($P = 0.025$, 0.0055, and 0.031, respectively). The latter also correlated with a longer PFS. The iPET DTTV SUV_{mean} obtained with the liver as a threshold and the ratio of mean SUV_{max} obtained from target lesions at iPET to baseline PET correlated with the therapy response ($P = 0.024$ and 0.048, respectively) but not PFS. From the multivariable analysis with adjustment for age, primary site, and Ki-67 index, the mean SUV_{max} ($P = 0.019$), ratio of the mean lesion SUV_{max} to the SUV_{max} in the liver ($P = 0.018$), ratio of the mean lesion SUV_{max} to the SUV_{max} in the spleen ($P = 0.041$), DTTV SUV_{mean} obtained with the liver ($P = 0.0052$), and skewness ($P = 0.048$) remained significant predictors of PFS. **Conclusion:** The degree of somatostatin receptor expression and tumor heterogeneity, as represented by several metrics in our analysis, were predictive of the therapy response or PFS. Changes in these parameters after the first cycle of peptide receptor radionuclide therapy did not correlate with clinical outcomes.

Key Words: ^{68}Ga-DOTATATE; PET/CT; neuroendocrine tumors; PRRT; response; survival

J Nucl Med 2021; 62:1406–1414
DOI: 10.2967/jnumed.120.256727

Neuroendocrine tumors (NETs) are uncommon malignancies with a documented population incidence of 6 or 7 per 100,000 in 2012 (*1*). The most common primary tumor sites are gastroenteropancreatic, but they may arise in the lungs, adrenal glands, and pituitary gland, among other locations (*2*). Most NETs overexpress somatostatin receptors (SSTRs) on the cell surface, allowing for SSTR-based imaging with ^{68}Ga-(DOTA)-peptide PET; in recent years, the latter technique has become the preferred imaging modality for diagnosis, staging, and selection of patients for peptide receptor radionuclide therapy (PRRT) (*3*).

Coupling β- or γ-emitting radionuclides (^{177}Lu or ^{90}Y) to somatostatin analogs allows radionuclide therapy for well-differentiated unresectable or metastatic tumors that are highly DOTA–somatostatin analog avid (*4*). Multiple studies, including a recent phase III randomized trial (NETTER-1), have shown favorable progression-free survival (PFS) and overall survival, with limited, acceptable side effects (*5–11*). In 1 of those studies, treatment of patients who had midgut NETs with ^{177}Lu-DOTATATE and octreotide long-acting release resulted in longer PFS and overall survival than treatment with octreotide long-acting release alone (*11*).

In July 2016, a prospective, multicenter trial was launched in Ontario, Canada, to assess the outcome of patients who had progressive metastatic NETs treated with individualized dosimetry-guided ^{177}Lu-DOTATATE therapy and who were provided access to PRRT with regulatory Health Canada oversight. A further aim

Received Sep. 15, 2020; revision accepted Jan. 20, 2021.
For correspondence or reprints, contact Ur Metser (ur.metser@uhn.ca).
Published online February 12, 2021.

of that trial was to evaluate the prognostic value of quantitative ^{68}Ga-DOTATATE PET/CT performed for patient selection. The purpose of the present study was to determine whether semiquantitative, volumetric, and tumor heterogeneity parameters on baseline PET (bPET) and early interim PET (iPET) performed before a second cycle of therapy are predictive of the therapy response and PFS.

MATERIALS AND METHODS

Study Design

Patients included in this analysis were enrolled in a prospective, multicenter, single-arm institutional review board–approved study (NCT02743741). All patients signed a written informed consent form. Eligibility criteria included biopsy-proven NET, with no restriction on primary site of origin; Ki-67 index of less than or equal to 30%; and progressive disease before study enrollment. All patients underwent screening with ^{68}Ga-DOTATATE PET/CT to confirm the adequate expression of SSTR type 2. In eligible patients, most tumor sites exhibited a high level of ^{68}Ga-DOTATATE uptake (defined as a Krenning score of 3 or 4) (*12*,*13*). An optional iPET scan was performed before cycle 2 of ^{177}Lu-DOTATATE therapy to explore its prognostic value for clinical outcomes. Associations between bPET or iPET parameters and the outcome measures (therapy response and PFS) were evaluated.

Study Procedure

^{68}Ga-DOTATATE PET/CT Imaging Protocol. PET was performed on a Siemens mCT40 PET/CT scanner (Siemens Healthcare). Patients were positioned supine with arms outside the region of interest. Images were obtained from the top of the skull to the upper thighs. Iodinated oral contrast material was administered for bowel opacification; no intravenous iodinated contrast material was used. Overall, 5–9 bed positions were obtained, depending on patient height, with an acquisition time of 2–3 min per bed position. A mean dose of 131.8 (SD = 29.7) MBq (range, 54.5–205 MBq) of ^{68}Ga-DOTATATE was administered, with a mean uptake time of 65.8 min (range, 50–93 min). CT parameters were 120 kV; 3.0 mm slice width, 2.0 mm collimation; 0.8 sec rotation time; 8.4 mm feed/rotation. A PET emission scan using time of flight with scatter correction was obtained covering the identical transverse field of view. PET parameters were as follows: image size: 2.6 pixels; slice: 3.27; and 5-mm full width at half maximum (FWHM) gaussian filter type. PET/CT images were reviewed on a dedicated nuclear medicine PACS system with fusion software (Mirada Medical). SUV measurements were obtained using a region of interest delineating selected tumor sites (Fig. 1).

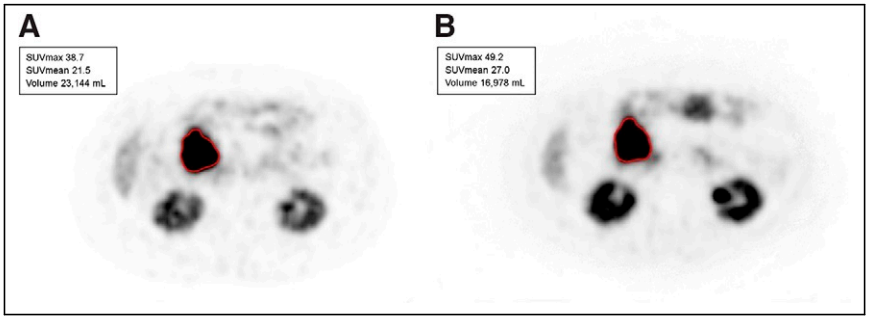

FIGURE 1. 60-y-old woman with metastases of well-differentiated small bowel NET to liver and retroperitoneal lymph nodes (G1; Ki-67 index, 6%). Lesion-based assessment was done with bPET and iPET before cycle 2 of ^{177}Lu-DOTATATE therapy. (A) Metastatic nodal mass chosen as marker lesion at bPET (SUV_{max}, 38.7) (outlined in red). (B) Same lesion before cycle 2 of therapy (SUV_{max}, 49.2) (outlined in red).

Tumor Volume Segmentation Software. A graphical user interface was developed in-house specifically to delineate whole-body tumor burden. An initial mask was defined by setting a threshold equal to the maximal value in a 3-dimensional volume of interest drawn within normal reference tissue, initially within the normal liver. From this general mask, normal physiologic tracer uptake was manually removed in a 3-dimensional maximum-intensity-projection space. The PET volume and the mask overlay were displayed at various radial angles, allowing the user to define and remove regions of normal uptake (e.g., myocardium, spleen, bladder) at any view, providing the clearest visible margins. Once the normal tissues were removed from the tumor mask, a final step allowed the user to manually add or subtract any other region to or from the mask. Correlation with morphologic imaging (contrast-enhanced CT or MRI) was performed when needed to ensure the accurate delineation of tumor sites. ^{68}Ga-DOTATATE tumor volumes (DTTVs), SUV_{max}, and SUV_{mean} were generated from the final tumor mask (Fig. 2). The same process was repeated with a threshold equal to the maximal value in a 3-dimensional volume of interest drawn within the normal spleen (a step-by-step demonstration of the segmentation process is provided in Supplemental Fig. 1 [supplemental materials are available at http://jnm.snmjournals.org]).

^{177}Lu-DOTATATE Therapy and Clinical Outcomes. Eligible patients were treated with 4 cycles of ^{177}Lu-DOTATATE or fewer if limited by toxicity or disease progression. Individualized dosimetry was used for the provision of ^{177}Lu-DOTATATE therapy. The initial administered activity of ^{177}Lu-DOTATATE was standardized at 7,400 MBq (200 mCi). Whole-body scintigraphy was performed at 4, 24, and 72 h after each cycle to estimate a recommended activity that will result in an accumulated absorbed dose to the kidneys of 23 Gy, with estimates of absorbed doses in the bone marrow and tumor. Dose escalation was capped at a maximum of 11,100 MBq (300 mCi) per dose. The final prescribed activity was determined by the treating physician on the basis of the recommended activity and patient factors, including renal and hematologic laboratory results. For the present report, the response to therapy was defined by the investigator on the basis of CT of the chest, abdomen, and pelvis performed 3 mo after the completion of therapy or earlier if disease progression was observed (*12*). Responders were defined as patients with a complete/partial response or stable disease, and nonresponders had progressive disease. Patients continued clinical and CT surveillance, and time to progression was documented for all study participants.

PET Data Abstraction

Reference Normal Tissue Values. The SUV_{max} in reference tissues, normal liver (lower threshold), and spleen (upper threshold) were recorded. In the liver, the SUV_{max} was measured in the posterior right lobe. For patients who underwent splenectomy, normal renal parenchyma was used for the upper threshold instead of the spleen (*12*,*13*). In the present report, both upper-threshold references are referred to collectively as "spleen."

Tumor Parameters. Three types of tumor parameters (marker lesion–based, whole-body DTTV, and first-order heterogeneity parameters) were assessed, for a total of 13 metrics from the baseline and before cycle 2 scans, when available.

For lesion-based parameters, reference background tracer uptake in normal liver and

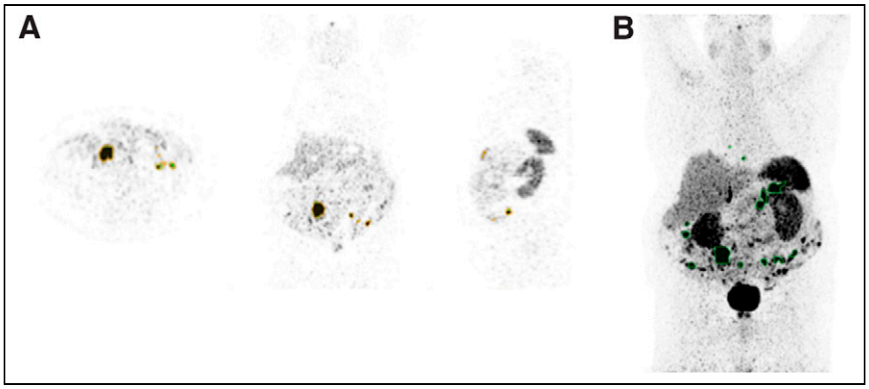

FIGURE 2. ^{68}Ga-DOTATATE tumor volume analysis using in-house automated segmentation software. (A) Multiplanar segmentation tool (to identify and confirm tumor sites). (B) Mask generated using tracer uptake in spleen as threshold (tumor lesions with SUV_{max} above that of spleen are outlined in green).

spleen tissues (or left renal cortex in the case of previous splenectomy) was measured (volumes of interest placed in the right hepatic lobe and spleen). Up to 5 well-defined, reproducible marker lesions larger than 1 cm were chosen, with no more than 2 lesions per disease site or organ, in accordance with RECIST 1.1 recommendations (*14*,*15*). The SUV_{max} of each lesion and the mean SUV_{max} of all marker lesions were recorded. In addition, the ratio of the lesion SUV_{max} to the SUV_{max} in the liver (SUV_{max} T/L) or the SUV_{max} in the spleen (SUV_{max} T/S) was calculated.

For DTTV parameters, the maximum SUV within the volume of interest drawn over the liver and spleen was used as a threshold for the measurement of DTTV in the liver and DTTV in the spleen. The total DTTV (DTTV with liver and spleen as thresholds), the SUV_{max} generated from the contoured volumes, and the SUV_{mean} generated for each threshold were documented.

TABLE 1
Patient Characteristics for Entire Cohort and Subgroup with iPET

Characteristic	Entire cohort	iPET cohort
No. of patients	91	36
Sex (M:F)	53:38	20:16
Mean age (y)	62.5 (SD = 12.9)	59.7 (SD = 14.2)
Primary site (No. of patients)		
Gastrointestinal tract	48	19
Pancreas	19	8
Unknown primary	9	2
Bronchopulmonary	6	3
Adrenal	4	2
Other	5	2
Mean tumor Ki-67 index (%)	8.3 (SD = 7.8)	10.5 (SD = 8.3)
Response status		
Nonresponders	20	6
Other	71	30
Mean follow-up (mo)	12.2 (SD = 7.2)	20.1 (SD = 9.7)

The heterogeneity of SSTR type 2 expression at the various tumor sites was assessed using the segmented 3-dimensional tumor volumes. For this purpose, 3 different first-order heterogeneity radiomics parameters were evaluated within the generated volumes: coefficient of variation, defined as the SD divided by the mean of the activity concentration in the tumor volume; skewness, the third standardized moment and measure of the asymmetry of the activity distribution at tumor sites; and kurtosis, the fourth standardized moment and measure of the "tailedness" of the probability distribution. For both skewness and kurtosis, the metrics were calculated with and without sample size bias correction, and no significant differences were observed.

Statistical Analysis

Summary statistics were used to describe patient and disease characteristics, with mean and range for continuous variables and frequency and percentage for categoric variables. Box plots were used to visualize the distribution of continuous variables between responders and nonresponders. A 2-sided Wilcoxon rank sum test was used to test for associations between continuous variables and the response. All markers for PFS, defined as survival without progression or death, were assessed using a univariable Cox proportional hazards model. Each statistically significant marker from the univariable analysis was further assessed using a multivariable Cox proportional hazards model with adjustment for patient factors, including age, primary disease site, and Ki-67 index. A P value of less than 0.05 was considered statistically significant, without adjustment for multiple comparisons.

RESULTS

Patient Demographics

At the time of data lock for the present analysis (December 2019), 96 consecutive subjects had been referred between August 2016 and January 2019 for consideration of PRRT. Five subjects who were not treated were excluded (2 withdrew from the study, and 3 had inadequate tracer uptake in tumor sites). Thus, 91 patients who fulfilled the inclusion criteria, received therapy, and had follow-up data available comprised the study cohort. Thirty-six of them underwent iPET. Patient characteristics are shown in Table 1. Patients received up to 4 cycles of PRRT (mean, 3.67: range, 1–4) with an average dose of 7,375.1 MBq (range, 972–12,659 MBq). The mean clinical follow-up was 12.2 mo (range, 1.4–38 mo). There were 71 responders (51 with stable disease; 20 with a partial response) and 20 nonresponders. The mean PFS was 18.9 mo (95% CI, 15.6–22.8 mo).

bPET Parameters

Reference Tissues. The SUV_{max} in 2 reference tissues, normal liver and spleen, were compared in responders and nonresponders. For 9 patients who underwent splenectomy, normal renal parenchyma was used instead of the spleen as the upper-threshold reference. For the lesion-based analysis, a mean of 4.7 target lesions was evaluated for each patient (median, 5; range, 2–5). Baseline reference tissue parameters (lesion-based ^{68}Ga-DOTATATE PET/CT measures, DTTV parameters, and

TABLE 2
bPET Reference Parameters, Lesion-Based Parameters, DTTV Parameters, and First-Order Heterogeneity Parameters

bPET Parameter	All Patients (n = 91)	Responders (n = 71)	Nonresponders (n = 20)	P*
Reference tissue				
SUV_{max} liver				0.49
Mean (SD)	5.7 (2.1)	5.8 (2.3)	5.3 (1.6)	
Minimum–maximum	2–13.1	3.2–8.2	2–13.1	
SUV_{max} spleen				0.30
Mean (SD)	13.8 (6.9)	14.1 (6.9)	12.6 (6.7)	
Minimum–maximum	4.4–45.8	4.4–26.7	5–45.8	
Lesion based				
Mean SUV_{max}				0.018
Mean (SD)	38.7 (25.1)	41.7 (26.8)	28.2 (14.2)	
Minimum–maximum	11–137.7	13.4–77.4	11–137.7	
Mean SUV_{max} T/L				0.024
Mean (SD)	8.3 (6.4)	9 (7)	5.8 (2.9)	
Minimum–maximum	1.4–40.5	1.4–40.5	2.9–14.6	
Mean SUV_{max} T/S				0.13
Mean (SD)	3.5 (2.7)	3.7 (2.9)	2.8 (1.8)	
Minimum–maximum	0.2–14.6	0.2–14.6	1–8.3	
DTTV				
DTTV liver†				0.12
Mean (SD)	554.1 (853.8)	611.5 (921.7)	350.4 (516.8)	
Minimum–maximum	4.7–4,891.8	4.7–4,891.8	8.1–2,200.9	
DTTV spleen†				0.06
Mean (SD)	317.1 (616.3)	363.9 (677.6)	150.9 (265.4)	
Minimum–maximum	0–3,825.3	0–3,825.3	0–1,049.6	
DTTV SUV_{max}				0.025
Mean (SD)	62.8 (46.4)	66.8 (48.4)	48.4 (36.2)	
Minimum–maximum	15.6–307)	17.1–307	15.6–186.6	
DTTV SUV_{mean} liver				0.0055
Mean (SD)	15.6 (7.3)	16.7 (7.7)	11.6 (3.6)	
Minimum–maximum	5.1–41.4	5.8–41.4	5.1–19.4	
DTTV SUV_{mean} spleen				0.06
Mean (SD)	23.5 (10.3)	24.5 (10.4)	20 (9.3)	
Minimum–maximum	0–50.4	0–50.4	7.7–45.3	
Heterogeneity				
CoV				0.17
Mean (SD)	0.6 (0.2)	0.6 (0.2)	0.6 (0.3)	
Minimum–maximum	0.2–1.6	0.3–1.5	0.2–1.6	
Skewness				0.055
Mean (SD)	1.5 (0.8)	1.4 (0.8)	1.9 (1.0)	
Minimum–maximum	0.1–4	0.1–4	0.6–4	
Kurtosis				0.031
Mean (SD)	6.4 (4.8)	5.8 (4.1)	8.6 (6.4)	
Minimum–maximum	1.7–26.7	1.7–25.8	2.8–26.7	

*P value.

†Measured in cubic centimeters.

DTTV SUV_{mean} liver = SUV_{mean} in segmented volume obtained with liver as threshold; DTTV SUV_{mean} spleen = SUV_{mean} in segmented volume obtained with spleen as threshold; DTTV liver = DTTV obtained with liver as threshold; DTTV spleen = DTTV obtained with spleen as threshold; DTTV SUV_{mean} liver = DTTV SUV_{mean} obtained with liver as threshold; DTTV SUV_{mean} spleen = DTTV SUV_{mean} obtained with spleen as threshold; CoV = coefficient of variation.

Wilcoxon rank sum test P values are shown.

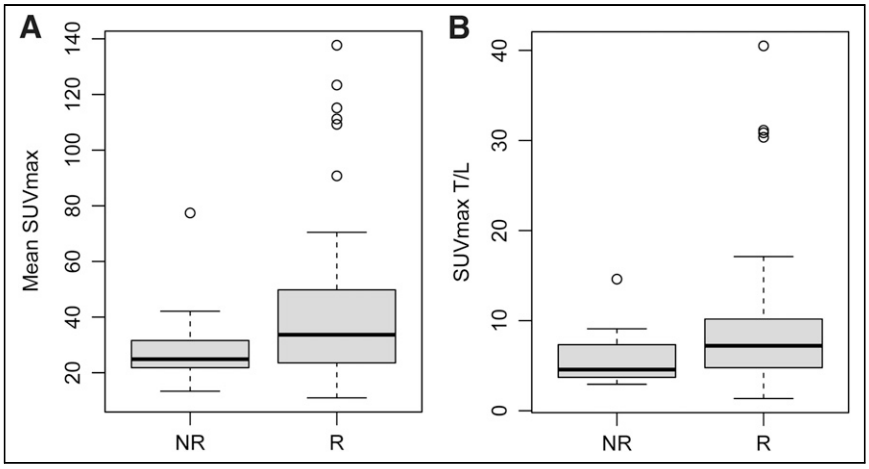

FIGURE 3. Lesion-based measures. Distributions of median SUV_{max} ($P = 0.018$) (A) and SUV_{max} T/L ($P = 0.024$) (B) are shown. Box plots represent median and upper and lower quartiles of each distribution, with whiskers showing limits of distribution (1.5 times interquartile range). NR = nonresponders; R = responders.

heterogeneity parameters) for responders and nonresponders are summarized in Table 2.

Tumor Parameters. For marker lesions, higher mean SUV_{max} and SUV_{max} T/L were predictive of the therapy response ($P = 0.018$ and 0.024, respectively) (Fig. 3). Similarly, higher SUV_{max} measured in DTTVs and SUV_{mean} of segmented tumor volumes with the liver used as a threshold were associated with the therapy response ($P = 0.025$ and 0.0055, respectively) (Fig. 4). An association of mean SUV_{max} of target lesions, SUV_{max} T/L, SUV_{max} T/S, and SUV_{mean} of segmented tumor volumes with the liver used as a threshold with progression or death was demonstrated ($P = 0.0023$. 0.028, 0.047, and 0.0053, respectively).

Of the 3 analyzed first-order heterogeneity parameters, only kurtosis emerged as a significant predictor of outcome, with higher values in nonresponders than in responders (Fig. 5). Both skewness (hazard ratio [HR], 1.49 [95% CI, 1.07–2.07]; $P = 0.017$) and kurtosis (HR, 1.06 [95% CI, 1.01–1.11]; $P = 0.022$) were associated with progression or death.

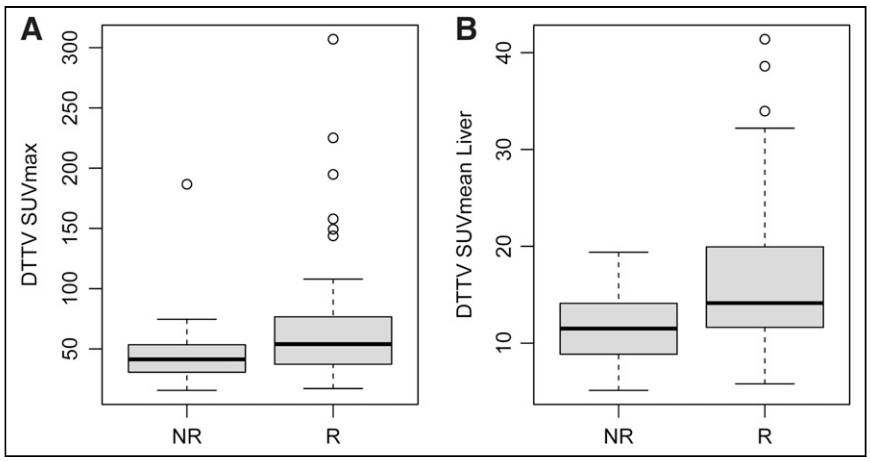

FIGURE 4. DTTV parameters. Distributions of mean DTTV SUV_{max} ($P = 0.025$) (A) and SUV_{mean} obtained with liver as threshold (SUV_{mean} Liver) ($P = 0.0055$) (B) are shown. Box plots represent median and upper and lower quartiles of each distribution, with whiskers showing limits of distribution (1.5 times interquartile range). NR = nonresponders; R = responders.

iPET Response Assessment Parameters

iPET lesion-based, DTTV, and heterogeneity parameters are shown in Table 3. Changes in the various parameters between bPET and iPET are shown in Supplemental Table 1.

PFS

There was a correlation of higher mean SUV_{max}, SUV_{max} T/L, SUV_{max} T/S, and DTTV SUV_{mean} obtained with the liver as a threshold with a longer PFS ($P = 0.023$, 0.028, 0.047, and 0.0053, respectively). Conversely, higher kurtosis and skewness were correlated with a shorter PFS ($P = 0.0022$ and 0.017, respectively).

From the multivariable analysis with adjustment for age, primary site, and Ki-67 index, the mean SUV_{max} ($P = 0.019$), SUV_{max} T/L ($P = 0.018$), SUV_{max} T/S ($P = 0.041$), DTTV SUV_{mean} obtained with the liver as a threshold ($P = 0.0052$), and skewness ($P = 0.048$) remained statistically significant predictors of PFS; however, variable kurtosis was not significant in the multivariable analysis. None of the analyzed parameters at iPET showed a statistical correlation with PFS in the univariable analysis.

Table 4 shows the results for the univariable analysis of the prediction of PFS from demographic data, the tumor Ki-67 index, lesion-based measures, DTTV parameters, and heterogeneity parameters on bPET as well as the multivariable analysis results obtained from statistically significant parameters in the univariable analysis when correlated with age, primary disease site, and Ki-67 index. The complete univariable analysis is shown in Supplemental Table 2.

DISCUSSION

The identification of biomarkers predictive of the therapy response and prognosis is essential for personalized care. PRRT is an effective mode of therapy in patients with metastatic NETs, but it is only appropriate for patients whose tumors highly overexpress somatostatin receptors (*16*). As would be expected and as previously reported, a higher tumor SUV_{max} on ^{68}Ga-DOTATATE PET/CT correlates with the treatment response (*17–20*). A few SUV-based parameters, including the mean SUV_{max} of target lesions and the SUV_{mean} generated from the DTTV with the liver as a threshold, were predictive of the response to PRRT; both the mean SUV_{max} and the DDTV SUV_{mean} obtained with the liver as a threshold also correlated with PFS (HRs, 1.04 and 1.19, respectively). A further interesting observation from the present study was that there was generally a higher SUV_{max} in reference tissues (normal liver and spleen) at iPET in patients who responded to PRRT. In the normal liver, SSTRs are predominantly found in

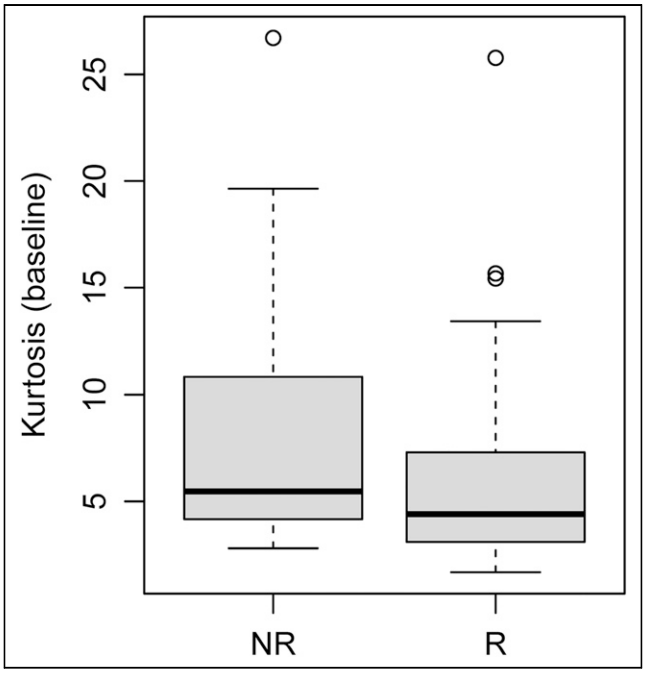

FIGURE 5. Kurtosis on baseline ^{68}Ga-DOTATATE PET/CT. Distribution of kurtosis was estimated from ^{68}Ga-DOTATATE tumor volumes (P = 0.031). Box plot represents median and upper and lower quartiles of each distribution, with whiskers showing limits of distribution (1.5 times interquartile range). NR = nonresponders; R = responders.

bile ducts, whereas in the normal spleen, autoradiography and immunohistochemistry studies have shown that they are found predominantly in red pulp (21,22). The reason for the presumed flare phenomenon in tracer uptake in normal tissues with a high level of expression of SSTRs is uncertain; however, it may reflect an inflammatory response, with an increase in activated macrophages that overexpress SSTR-1 and SSTR-2 on their cell surface (23,24). This phenomenon has also been the basis of imaging of inflammation in atherosclerosis and myocarditis with ^{68}Ga-DOTATATE PET/CT (25,26).

Early prediction of treatment failure can be a powerful clinical tool. For certain disease entities, early biomarkers have been validated and are clinically used to tailor therapy and reduce toxicity. Although generally well tolerated, PRRT can be associated with significant hematologic, renal, and hepatic toxicities (in approximately 10%, 0.4%, and 0.4% of patients, respectively) (*27*). Despite the high radiation dose delivered, disease progression is observed in 20%–30% of patients, and most patients achieve stable disease as the best response (*28*). Biomarkers that accurately predict PRRT outcomes may identify patients who are unlikely to benefit from it and limit unnecessary toxicity. Although the SUV_{mean} generated from the DTTV with the liver as a threshold on iPET was significantly higher in responders than in nonresponders (18.1 [SD = 9.1] and 11.2 [SD = 3.3], respectively), the overlap may limit the clinical utility of this observation.

NETs often exhibit intratumoral heterogeneity. Skewness and kurtosis, first-order features of heterogeneity, depict the asymmetry within the gray-level distribution observed within a

TABLE 3
iPET Reference Parameters, Lesion-Based Parameters, DTTV Parameters, and First-Order Heterogeneity Measures, Part 1

iPET	All patients (n = 36)	Responders (n = 30)	Nonresponders (n = 6)	P*
Reference tissue				
SUV_{max} liver				0.011
Mean (SD)	5.8 (1.8)	6.1 (1.8)	4.2 (1.2)	
Minimum–maximum	2.8–11.2	3.6–11.2	2.8–6.4	
SUV_{max} spleen				0.0085
Mean (SD)	19.4 (10.6)	21.2 (10.7)	10.6 (3.8)	
Minimum–maximum	4.3–49.1	7.3–49.1	4.3–14.6	
Lesion based				
Mean SUV_{max}				0.048
Mean (SD)	34.3 (19.4)	37 (20.2)	21.2 (6)	
Minimum–maximum	6.8–93.1	6.8–93.1	12.4–29.9	
Mean SUV_{max} T/L				0.57
Mean (SD)	6.1 (3.2)	6.3 (3.5)	5.2 (1.4)	
Minimum–maximum	0.9–17.4	0.9–17.4	2.9–6.8	
Mean SUV_{max} T/S				0.92
Mean (SD)	2.1 (1.2)	2.1 (1.3)	2.2 (0.9)	
Minimum–maximum	0.1–6.1	0.1–6.1	1.5–3.9	

*P value.

†Measured in cubic centimeters.

DTTV SUV_{mean} liver = SUV_{mean} in segmented volume obtained with liver as threshold; DTTV SUV_{mean} spleen = SUV_{mean} in segmented volume obtained with spleen as threshold; DTTV liver = DTTV obtained with liver as threshold; DTTV spleen = DTTV obtained with spleen as threshold; DTTV SUV_{mean} liver = DTTV SUV_{mean} obtained with liver as threshold; DTTV SUV_{mean} spleen = DTTV SUV_{mean} obtained with spleen as threshold; CoV = coefficient of variation.

Wilcoxon rank sum test P values are shown.

TABLE 3
iPET Reference Parameters, Lesion-Based Parameters, DTTV Parameters, and First-Order Heterogeneity Measures, Part 2

iPET	All patients (n = 36)	Responders (n = 30)	Nonresponders (n = 6)	P*
DTTV				
DTTV liver†				0.66
Mean (SD)	332.7 (424.6)	343.9 (438.8)	276.9 (375.1)	
Minimum–maximum	6–1,897.1	6–1,897.1	11.6–979.8	
DTTV spleen†				0.85
Mean (SD)	158.7 (256.3)	163 (270.1)	137.1 (189.9)	
Minimum–maximum	0–1,182.8	0–1,182.80	7.2–452.9	
DTTV SUV_{max}				0.11
Mean (SD)	58.8 (37.2)	63 (39.3)	38.1 (11.1)	
Minimum–maximum	16.9–197.5	16.9–197.5	25.8–55.1	
DTTV SUV_{mean} liver				0.024
Mean (SD)	16.9 (8.7)	18.1 (9.1)	11.2 (3.3)	
Minimum–maximum	5.7–50.7	5.7–50.7	6.3–16.6	
DTTV SUV_{mean} spleen				0.071
Mean (SD)	25.1 (12.6)	26.6 (13)	17.5 (7.9)	
Minimum–maximum	0–50.7	0–50.7	8–31.5	
Heterogeneity				
CoV				0.47
Mean (SD)	0.6 (0.2)	0.6 (0.2)	0.6 (0.1)	
Minimum–maximum	0.3–0.9	0.3–0.9	0.5–0.7	
Skewness				0.95
Mean (SD)	1.4 (0.8)	1.4 (0.8)	1.4 (0.8)	
Minimum–maximum	0.2–3.3	0.2–3.3	0.6–2.5	
Kurtosis				0.82
Mean (SD)	6.1 (4.1)	6.1 (4)	6.3 (5)	
Minimum–maximum	1.8–18.3	1.8–18.3	2.6–14.3	

*P value.

†Measured in cubic centimeters.

DTTV SUV_{mean} liver = SUV_{mean} in segmented volume obtained with liver as threshold; DTTV SUV_{mean} spleen = SUV_{mean} in segmented volume obtained with spleen as threshold; DTTV liver = DTTV obtained with liver as threshold; DTTV spleen = DTTV obtained with spleen as threshold; DTTV SUV_{mean} liver = DTTV SUV_{mean} obtained with liver as threshold; DTTV SUV_{mean} spleen = DTTV SUV_{mean} obtained with spleen as threshold; CoV = coefficient of variation.

Wilcoxon rank sum test P values are shown.

volume of interest and spreading of the expected gaussian curve, respectively. We have shown an inverse relationship between the baseline measurement of kurtosis and the response to PRRT. Both measured parameters correlate inversely with PFS (HRs, 0.54 and 0.9, respectively). These findings are in line with those of previous studies showing the predictive value of the subjective assessment of tumor heterogeneity and the response to PRRT (*29–31*). Graf et al. recently reported that the visual assessment of SSTR heterogeneity had both predictive value and prognostic value in progressive grade 1 or grade 2 NET patients undergoing PRRT, exceeding the prognostic value of the Ki-67 index (*31*).

There are several limitations of the present study. First, we included patients with multiple different NET sites, as the study was designed to enable broad access to PRRT for patients with metastatic NETs. However, patient selection criteria, including the Ki-67 index and SSTR type 2 expression on PET, were standardized. Second, iPET was optional and was performed only for a subset of patients. However, iPET parameters added little to patient outcomes and were not predictive of PFS. Third, DTTV and quantitative heterogeneity parameters required the use of segmentation tools, some of which are time-consuming and may not be practical for routine clinical use. However, we have shown that manual SUV_{max} measurements of target lesion can be used. Furthermore, a previous publication suggested that the subjective evaluation of heterogeneity has prognostic value, and some of our objective measures of tumor heterogeneity confirm this observation (*31*). Fourth, there was an overlap between responders and nonresponders for all of the predictive parameters, including parameters after cycle 1 of PRRT, limiting their clinical utility in isolation for guiding patient management.

TABLE 4
Univariable (UVA) and Multivariable (MVA) Analyses of Lesion-Based, Tumor Volume–Based, and Heterogeneity Parameters as Predictors of PFS

	UVA		MVA	
bPET covariate	HR (95% CI)	*P*	HR (95% CI)	*P*
Lesion based				
Mean SUV_{max}	0.98 (0.97–1)	0.023	0.98 (0.96–1)	0.019
SUV_{max} T/L	0.92 (0.85–0.99)	0.028	0.89 (0.8–0.98)	0.018
SUV_{max} T/S	0.86 (0.75–1)	0.047	0.83 (0.69–0.99)	0.041
Tumor volume				
DTTV SUV_{mean} liver	0.92 (0.87–0.98)	0.0053	0.9 (0.83–0.97)	0.0052
Heterogeneity				
Skewness	1.49 (1.07–2.07)	0.017	1.48 (1–2.18)	0.048

DTTV SUV_{mean} liver = SUV_{mean} from tumor volume obtained with liver or spleen as threshold.
Cox proportional hazards model *P* values are shown.

CONCLUSION

The degree of SSTR type 2 expression and tumor heterogeneity, as represented by several metrics in our analysis, are predictive of the therapy response or PFS. Changes in these parameters after cycle 1 of PRRT did not correlate with clinical outcomes. A model or scoring system integrating combinations of the predictive parameters identified with other clinical prognostic factors should be developed to predict the therapy response and patient outcomes more reliably.

DISCLOSURE

Funding was provided by the Ontario Health-Cancer Care Ontario Neuroendocrine Tumor Consortium to run the trial at the local sites as well as for central trial coordination. Funding was also provided by the Princess Margaret Hospital Foundation to support central trial coordination. In addition, funding was provided by the Susan Leslie Clinic for Neuroendocrine Tumors, Odette Cancer Centre, to support the implementation of the trial at Odette Cancer Center. No other potential conflict of interest relevant to this article was reported.

KEY POINTS

QUESTION: Are there quantitative ^{68}Ga-DOTATATE parameters at bPET or iPET after 1 cycle of PRRT that are predictive of the response to therapy, PFS, or both?

PERTINENT FINDINGS: Higher SUV_{max} in marker tumor sites and SUV_{mean} of segmented DTTVs obtained with the liver as a threshold at bPET and iPET correlated with the therapy response, and the baseline parameters were predictive of PFS. Skewness, a first-order feature of tumor heterogeneity, was also associated with PFS, and changes observed at iPET did not correlate with outcomes.

IMPLICATIONS FOR PATIENT CARE: Although certain quantitative ^{68}Ga-DOTATATE PET parameters are predictive of a response to PRRT and PFS, the overlap of these parameters in responders and nonresponders limits their clinical utility in isolation for guiding patient management.

REFERENCES

1. Dasari A, Shen C, Halperin D, et al. Trends in the incidence, prevalence, and survival outcomes in patients with neuroendocrine tumors in the United States. *JAMA Oncol.* 2017;3:1335–1342.
2. National Comprehensive Cancer Network. NCCN Clinical Practice Guidelines in Oncology: Neuroendocrine Tumors Version 1.2013. https://www.nccn.org/professionals/physician_gls/pdf/neuroendocrine_blocks.pdf. Accessed September 17, 2021.
3. Hope TA, Bergsland EK, Bozkurt MF, et al. Appropriate use criteria for somatostatin receptor PET imaging in neuroendocrine tumors. *J Nucl Med.* 2018;59:66–74.
4. Bodei L, Kidd M, Modlin IM, et al. Measurement of circulating transcripts and gene cluster analysis predicts and defines therapeutic efficacy of peptide receptor radionuclide therapy (PRRT) in neuroendocrine tumors. *Eur J Nucl Med Mol Imaging.* 2016;43:839–851.
5. Kwekkeboom DJ, Teunissen JJ, Bakker WH, et al. Radiolabeled somatostatin analog [^{177}Lu-DOTA0, Tyr3]octreotate in patients with endocrine gastroenteropancreatic tumors. *J Clin Oncol.* 2005;23:2754–2762.
6. Kwekkeboom DJ, de Herder WW, Kam BL, et al. Treatment with the radiolabeled somatostatin analog [^{177}Lu-DOTA0, Tyr3]octreotate: toxicity, efficacy, and survival. *J Clin Oncol.* 2008;26:2124–2130.
7. Kwekkeboom DJ, Kam BL, van Essen M, et al. Somatostatin-receptor-based imaging and therapy of gastroenteropancreatic neuroendocrine tumors. *Endocr Relat Cancer.* 2010;17:R53–R73.
8. Imhof A, Brunner P, Marincek N, et al. Response, survival, and long-term toxicity after therapy with the radiolabeled somatostatin analogue [^{90}Y-DOTA]-TOC in metastasized neuroendocrine cancers. *J Clin Oncol.* 2011;29:2416–2423.
9. Baum RP, Kulkarni HR, Singh A, et al. Results and adverse events of personalized peptide receptor radionuclide therapy with ^{90}Yttrium and ^{177}Lutetium in 1048 patients with neuroendocrine neoplasms. *Oncotarget.* 2018;9:16932–16950.
10. Hörsch D, Ezziddin S, Haug A, et al. Effectiveness and side-effects of peptide receptor radionuclide therapy for neuroendocrine neoplasms in Germany: a multi-institutional registry study with prospective follow-up. *Eur J Cancer.* 2016;58:41–51.
11. Strosberg J, El-Haddad G, Wolin E, et al. Phase 3 trial of ^{177}Lu-Dotatate for midgut neuroendocrine tumors. *N Engl J Med.* 2017;376:125–135.
12. Krenning EP, Valkema R, Kooij PP, et al. Scintigraphy and radionuclide therapy with [indium-111-labelled-diethyl triamine penta-acetic acid-D-Phe1]-octreotide. *Ital J Gastroenterol Hepatol.* 1999;31(suppl 2):S219–S223.
13. Hope TA, Calais J, Zhang L, Dieckmann W, Millo C. ^{111}In-pentetreotide scintigraphy versus ^{68}Ga-DOTATATE PET: impact on Krenning scores and effect of tumor burden. *J Nucl Med.* 2019;60:1266–1269.
14. Wahl RL, Jacene H, Kasamon Y, Lodge MA. From RECIST to PERCIST: evolving considerations for PET response criteria in solid tumors. *J Nucl Med.* 2009;50(suppl 1):122S–150S.
15. Eisenhauer EA, Therasse P, Bogaerts J, et al. New response evaluation criteria in solid tumours: revised RECIST guideline (version 1.1). *Eur J Cancer.* 2009;45:228–247.

16. de Jong M, Breeman WA, Kwekkeboom DJ, Valkema R, Krenning EP. Tumor imaging and therapy using radiolabeled somatostatin analogues. *Acc Chem Res.* 2009;42:873–880.
17. Haug AR, Auernhammer CJ, Wängler B, et al. ^{68}Ga-DOTATATE PET/CT for the early prediction of response to somatostatin receptor–mediated radionuclide therapy in patients with well-differentiated neuroendocrine tumors. *J Nucl Med.* 2010; 51:1349–1356.
18. Miederer M, Seidl S, Buck A, et al. Correlation of immunohistopathological expression of somatostatin receptor 2 with standardised uptake values in ^{68}Ga-DOTATOC PET/CT. *Eur J Nucl Med Mol Imaging.* 2009;36:48–52.
19. Campana D, Ambrosini V, Pezzilli R, et al. Standardized uptake values of ^{68}Ga-DOTANOC PET: a promising prognostic tool in neuroendocrine tumors. *J Nucl Med.* 2010;51:353–359.
20. Kratochwil C, Stefanova M, Mavriopoulou E, et al. SUV of [^{68}Ga]DOTATOC-PET/CT predicts response probability of PRRT in neuroendocrine tumors. *Mol Imaging Biol.* 2015;17:313–318.
21. Reynaert H, Rombouts K, Vandermonde A, et al. Expression of somatostatin receptors in normal and cirrhotic human liver and in hepatocellular carcinoma. *Gut.* 2004;53:1180–1189.
22. Sarikaya I, Sarikaya A, Alnafisi N, Alenezi S. Significance of splenic uptake on somatostatin receptor imaging studies. *Nucl Med Rev Cent East Eur.* 2018; 21:66–70.
23. Dalm VA, van Hagen PM, van Koetsveld PM, et al. Expression of somatostatin, cortistatin, and somatostatin receptors in human monocytes, macrophages, and dendritic cells. *Am J Physiol Endocrinol Metab.* 2003;285:E344–E353.
24. Armani C, Catalani E, Balbarini A, Bagnoli P, Cervia D. Expression, pharmacology, and functional role of somatostatin receptor subtypes 1 and 2 in human macrophages. *J Leukoc Biol.* 2007;81:845–855.
25. Li X, Bauer W, Kreissl MC, et al. Specific somatostatin receptor II expression in arterial plaque: ^{68}Ga-DOTATATE autoradiographic, immunohistochemical and flow cytometric studies in apoE-deficient mice. *Atherosclerosis.* 2013;230:33–39.
26. Lapa C, Reiter T, Li X, et al. Imaging of myocardial inflammation with somatostatin receptor based PET/CT: a comparison to cardiac MRI. *Int J Cardiol.* 2015; 194:44–49.
27. Lin E, Chen, T, Little A, et al. Safety and outcomes of ^{177} Lu-DOTATATE for neuroendocrine tumours: experience in New South Wales, Australia. *Intern Med J.* 2019;49:1268–1277.
28. Marusyk A, Polyak K. Tumor heterogeneity: causes and consequences. *Biochim Biophys Acta.* 2010;1805:105–117.
29. Werner RA, Ilhan H, Lehner S, et al. Pre-therapy somatostatin receptor-based heterogeneity predicts overall survival in pancreatic neuroendocrine tumor patients undergoing peptide receptor radionuclide therapy. *Mol Imaging Biol.* 2019;21: 582–590.
30. Wetz C, Apostolova I, Steffen IG, et al. Predictive value of asphericity in pretherapeutic [^{111}In]DTPA-octreotide SPECT/CT for response to peptide receptor radionuclide therapy with [^{177}Lu]DOTATATE. *Mol Imaging Biol.* 2017; 19:437–445.
31. Graf J, Pape U, Jann H, et al. Prognostic significance of somatostatin receptor heterogeneity in progressive neuroendocrine tumor treated with Lu-177 DOTATOC or Lu-177 DOTATATE. *Eur J Nucl Med Mol Imaging.* 2020;47:881–894.